Observation of the segregation and the dissolution of the Co and the Cu in CoCu metastable alloys

M.L. Fdez-Gubieda,[a]* A. García Prieto,[a] A. García Arribas,[a] C. Meneghini[b] and S. Mobilio[b]

[a]Departamento de Electricidad y Electrónica. Universidad del País Vasco. Apartado 644, 48080 Bilbao. Spain, and [b]Laboratori Nazionali de Frascati (INFN), I-00044 Frascati. Italy. E-mail: malu@we.lc.ehu.es

Metastable Co_xCu_{100-x} ($x = 5, 10, 15, 20$) alloys have been annealed at increasing temperatures in order to study the evolution of the Co cluster and its relation with the magnetotransport properties. The structure was investigated by X-ray Absorption Spectroscopy on the Co K-edge as a function of composition and annealing temperature. An anomalous trend in the structural evolution has been evidenced and related to the peculiar features observed in the magnetotransport properties.

1. Introduction

Granular magnetic systems formed by magnetic clusters (e.g., Co) embedded in a non magnetic matrix (e.g., Cu) can present giant magnetoresistance effect (GMR). Co and Cu are inmiscible elements but a metastable CoCu solid solution can be prepared by rapid solidification techniques such as sputtering, electrodeposition, laser ablation, mechanical alloying and melt-spinning . After preparation, a thermal treatment provokes the segregation of the components in such a way that Co magnetic clusters are formed in the Cu matrix and the system presents GMR. In granular alloys, the magnetoresistance comes mainly from the spin-dependent scattering at the interfaces between the granules and the matrix (Berkowitz *et al.*, 1992; Xiao *et al.*, 1992; Zhang & Levy, 1993) and depends strongly on the size of magnetic particles, composition, as well as on the degree of interaction between them (Allia *et al.*, 1995; Wang *et al.*, 1998). All these parameters are controlled by the thermal treatment so a deep knowledge of the structural modification induced by the annealing is a fundamental issue to fully control the effect on the magnetoresistance.

The Co_xCu_{100-x} system has been extensively studied in the last years and the magnetic and magnetotransport properties as a function of annealing temperature are well known (Yu *et al.*, 1996; Viegas *et al.*, 1995). In fact, magnetic and magnetotransport measurements point that these systems present superparamagnetic behavior that arises from magnetic particles size of around 20Å. The presence of these small particles is responsible of the GMR.

However, there are not yet conclusive results that clarify what is the relation between the microstructure and the GMR and how it evolves with the thermal treatment. This lack of experimental evidence has its origin in the shortcomings of conventional techniques like X-ray diffraction and transmission electron microscopy with resolving such small structure.

The Extended X-ray Absorption Fine Structure (EXAFS) is an atom sensitive technique and very sensitive to the short range order around the absorber atom. EXAFS spectroscopy on the Co K-edge has allowed us to study the evolution of the surroundings of the Co atom in Co-Cu granular alloys with the thermal treatment. EXAFS analysis clearly evidences a peculiar trend in the structural evolution of the alloys as a function of the thermal treatment that has been related with the maximum of the GMR found after annealing at 723K.

2. Experimental techniques

Co_xCu_{100-x} ($x = 5, 10, 15, 20$) samples were prepared by rapid quenching in the form of long ribbons. Different pieces of each sample were submitted to thermal treatment at increasing temperatures ($T_{ann} = 673, 723, 773, 823, 873, 923$K) in an Ar controlled atmosphere furnace. The samples were checked by X-ray diffraction to be sure that they were oxide-free, as the oxidation completely changes the properties of the material. The very same piece of sample was used for magnetotransport and structural studies.

The MR has been measured using the conventional four points configuration at 10K in a SQUID magnetometer and with a magnetic field up to 7 T in order to achieve the saturation of the MR curve ($\mathrm{MR} = \frac{R(0)-R(H)}{R(0)}(\%)$).

EXAFS measurements on the Co K-edge, for samples $x = 5, 15$ and 20, were performed on the GILDA (Pascarelli *et al.*, 1996) beamline at the ESRF at 77 K in transmission geometry. The spectra of the $x = 10$ sample were collected at room temperature in the 7.1 station at the Daresbury Synchrotron Radiation Source (SRS).

3. Data analysis and results

In Figure 1 we present the evolution of the MR with the applied magnetic field for the as quenched and the annealed samples for $Co_{10}Cu_{90}$. We have found that in all the samples, regardless of the composition, the GMR presents its maximum value after annealing at 723K, the same result has been reported by other authors (Viegas *et al.*, 1997; Yu *et al.*, 1996).

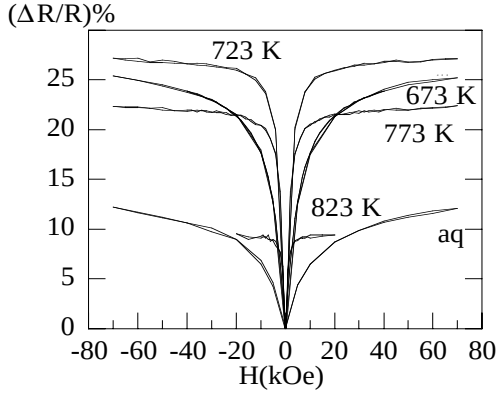

Figure 1
Giant magnetoresistance as a function of a magnetic field for as quenched and annealed $Co_{10}Cu_{90}$ samples measured at 10K.

The structural EXAFS (Extended X-ray Absorption Fine Structure) signals were extracted from absorption spectra using standard procedures for background substraction and data normalization (Lengeler & Eisenberger, 1980). Systematical errors were minimized using the same procedure for all the data sets.

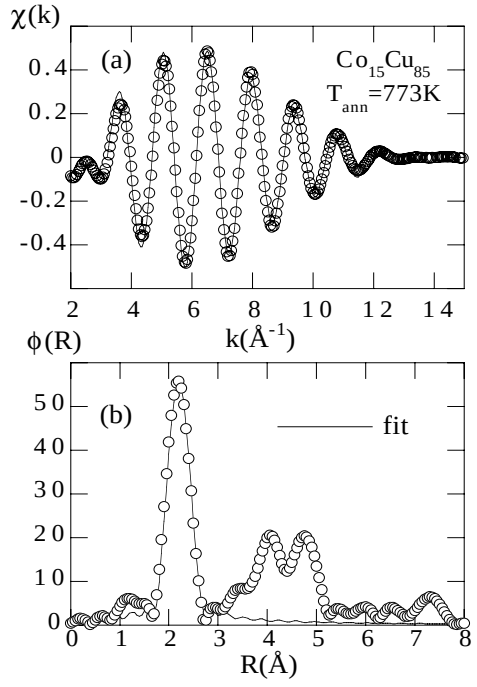

Figure 2
Co K-edge EXAFS experimental and theoretical function for $Co_{15}Cu_{85}$ annealed at 773K, showing the quality of the fit in (a) *k* and (b) *R* space.

The nearest neighbor contributions were isolated using the standard Fourier Filtering technique and the filtered data were fitted using the standard EXAFS formula (Stern, 1988):

$$k\chi(k) = \sum_j S_0^2 N_j f_j(k,\pi) \frac{e^{-2\sigma_j^2 k^2} e^{-2\Gamma_j/k}}{R_j^2} \sin[2kR_j + \phi_j] \qquad (1)$$

that represents the contribution of N neighbors distributed on a spheric shell of average radius R and variance σ around the absorber. The parameters $f_j(k,\pi)$ and ϕ_j are respectively the backscattering amplitude and phase shift. The scale factor S_0^2 is related to the many body effects and the Γ_j is the mean free path for the photoelectron. Since Co and Cu neighbors are almost indistinguishable as backscatterers, we have used a single shell model. The backscattering function $f_j(k,\pi)$ and ϕ_j, were extracted from an experimental EXAFS spectrum of pure fcc Co sample collected at 77K. The use of experimental amplitude and phase functions reduces the number of fitting parameters since S_0^2 and Γ_j are automatically included in the experimental amplitude function, this improves the best fit quality and the reliability of the results. Conventional X-ray diffraction has allowed us to know that the magnetic cluster, well observed after annealed at a high temperature, $T_{ann} = 923$K, presents a fcc structure. Since the coordination number is expected not to vary as a function of thermal treatment, N was fixed to 12 as expected in a fcc structure, this gives a higher reliability to the values of σ^2 obtained. It is worth to notice that the experimental amplitude also contains implicitely the Debye-Waller factor, σ^2_{fcc-Co}, thus the fitting gives relative values, being σ^2 the difference between the value of the Debye-Waller factor in the sample and in the model (fcc Co). The error bar in each parameter (± 0.005 Å for the interatomic distance, R, and 10% for the Debye-Waller factor, σ) is obtained using the MINOS command of MINUIT (James, 1994) taking into account for effects of correlations between the parameters. In Figure 2, we present the fit of one of the samples in *k* and *R* space.

We have also obtained the scattering parameters through a theoretical model using the FEFF (version 6.0) codes (Zabinsky *et al.*, 1995). In this case, we fitted the data up to 3 Å with the FEFFIT program and using multiple scattering theory (Newville *et al.*, 1993). The fitting was performed in the *R* range and in the analysis we considered that the reduced amplitude factor, S_0^2, and the edge energy correction were the same for each set of thermal treated samples with the same composition.

In Figure 3, we present the interatomic distance, R, and the Debye-Waller factor, σ^2, obtained with both fitting procedures as a function of annealing temperature, T_{ann}, and composition. The discrepancy between both fittings is presented as an error bar.

The very same evolution of both parameters has been found with both fitting methods so we can be really confident of the presented results.

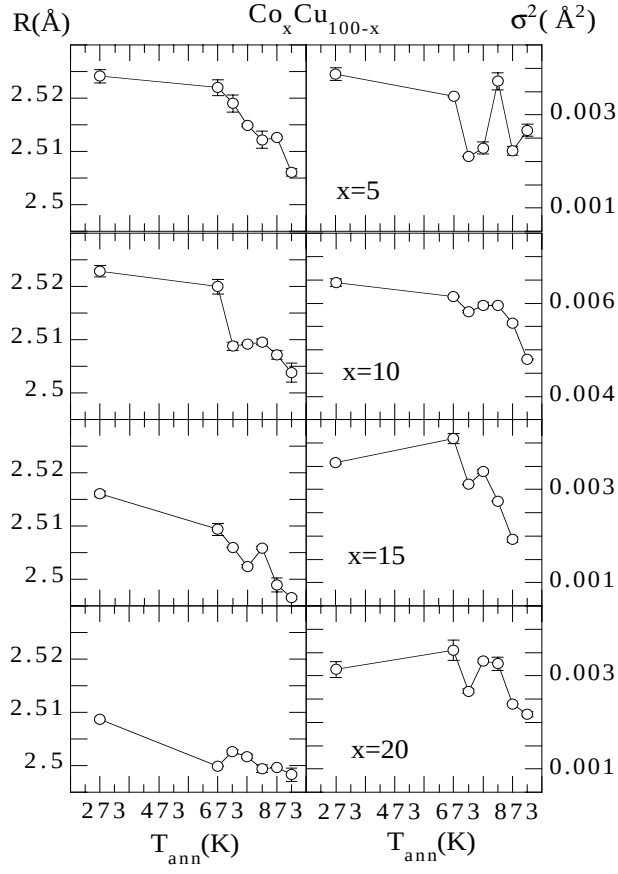

Figure 3
(a) Interatomic distance around the Co atom, R, (b) Debye-Waller factor for Co_xCu_{100-x} granular alloys measured at 77K except for $x = 10$, measured at room temperature. The error bars display the discrepancy between both fitting methods as explained in the text.

4. Discussion and conclusions

As can be observed in Figure 3, the interatomic distance around the Co atoms, R, for all the as-quenched samples presents a value higher than that of a pure fcc Co, (R = 2.492 Å at 77K). With increasing the annealing temperature, T_{ann}, the interatomic distance decreases. The same trend presents the Debye-Waller factor, that

in general decreases with T_{ann}. In a binary metallic alloy, A_xB_{1-x}, the bond lengths R_x are usually related to the bond lengths of each compounds R_A (x=1) and R_B (x=0) through: $R_x = xR_A + (1-x)R_B$ following the Vergard's law. This fact allows us to interpret the overall decreasing tendency of the bond lengths as an indicative of a progressive Co segregation as a function of annealing temperature. The Co atoms expulse the Cu atom from their environment and get together with other Co atoms, consequently the interatomic distance decreases, the chemical disorder around the Co diminishes and the Debye-Waller factor decreases.

But a more profound insight in Figure 3, clearly points a more complex behavior, the decreasing tendency is not monotonous and a clear structure in the curves is observed.

For the interatomic distance, the effect is difficult to analyze since it depends strongly on sample composition. In fact, for the samples with $x = 5$ composition the interatomic distance around the Co atom is strongly affected by the Cu matrix, while for the $x = 20$ ones, even in the as-quenched sample, the interatomic distance presents a value close to fcc Co which clearly indicates that large Co segregation, even before the thermal treatment, is present in the sample and the effect of the segregation is worth seen.

However, the Debye-Waller factor clearly presents an anomalous feature for the samples annealed between 723-823K, regardless of the composition. The decreasing tendency of this parameter is interrupted at 723K and slightly increases up to 823K. For the $x = 10$ samples, the Debye-Waller factor presents the highest value, since the spectra were measured at room temperature, so the contribution due to thermaly activated phonons is added to the Debye-Waller factor coming from structural disorder, and this partially masks the effect of annealing.

The different stages found with the thermal treatment, have been interpreted in the following way: from the as-quenched to the annealed at 723K, the reduction of the average distance and of the disorder is an indicative of the expulsion of the minority Cu atoms from the surroundings of the Co atoms, that must be joining toghether at the interfaces that are being formed. Small quite pure Co clusters are forming, surrounded by the interfaces where the expulsed Cu atoms are getting togheter. It is at this point where the conditions for a giant magnetoresistance are given: small particles, with well defined interfaces.

After annealing at temperatures higher than 723K, 723K $< T_{ann} <$ 823K, the disorder grows, or at least does not continue decreasing at the same rate. Note that at the very same annealing temperature the GMR starts to decrease.

All this features occur at the same annealing temperature for all the samples regardless of the composition. And it is not an artifact of data analysis as the same results are found using both types of fitting described above. To account for this event we must realize that at 773K a non negligible amount, less than 1%, of Cu begins to be accepted in the Co, according with the equilibrium phase diagram (Nishizawa & Ishidam, 1984). For this reason, the Cu atoms at the surroundings of the Co atom can readily be partially reincorporated in the Co granule, at least in the surface proximity. This explains the increase of the disorder around Co atoms, and also the breaking of the good magnetoresistance condition, having small Co particles with less sharp interfaces. Finally, the annealing at temperatures higher than 823K, makes definitive the segregation of Co atoms from the Cu rich phase.

We can conclude that different stages in the segregation of the Co have been found with the annealing temperature that are related to the magnetotransport behavior:

1. From the as-quenched to the annealed at 723K starts the segregation of the Co atoms. This process creates small Co particles surrounded by Cu with well defined interfaces and coincides with the point when the GMR reaches the maximum value.
2. At higher annealing temperature, 723K $< T_{ann} <$ 823K, an inverse process begins. According with the phase diagram, the solubility of Cu in Co begins to be finite at 773K, thus the sharp interface around Co particles that has been created diffuses and the GMR diminishes.
3. At higher temperature, $T_{ann} \geq$ 823K the Co follows its segregation and evolves to pure fcc Co.

Acknowledgements

This work has been supported by the Spanish CICyT under Projects No. MAT99-0667.

References

Allia, P., Knobel, M., Tiberto, P. & Vinai, F. (1995). *Phys. Rev. B* **52**, 15398–15411.
Berkowitz, A.E., Mitchell, J.R., Carey, M.J., Young, A.P., Zhang, S., Spada, F.E., Parjer, F.T., Hutten, A. & Thomas, G. (1992). *Phys. Rev. Lett.* **68**, 3745–3748.
James, F. (1994). *MINUIT: Function Minimization and Error Analysis. Reference manual (Version 94.1)*, Program library D506. CERN
Lengeler, B. & Eisenberger, P. (1980). *Phys. Rev. B* **21**, 4507–4512.
Nishizawa, T. & Ishidam, K. (1984). *Bul. Alloy Phase Diagrams* **5**, 161–161.
Pascarelli, S., Boscherini, F., D'Acapito, F., Hardy, J., Meneghini, C. & S. Mobilio, S. (1996). *J. Synchrotron Radiat.* **3**, 147–155.
Stern, E.A. (1988). *X-ray Absorption: Principles, Applications, Techniques of EXAFS, SEXAFS and XANES*, edited by D.C. Koningsberger & R. Prins, p.45. Wiley, New York
Stern, E.A., Newville, M., Ravel, B., Yakovy, Y. & Haskel, D. (1995). *Physica B* **208&209**, 117–125.
Viegas A.D.C., Geshev J., Dornless L.S., Schmidt J.E. & Knobel M.,(1997). *J. Appl. Phys.* **82**, 3047–3053.
Wang, W., Zhu, F., Weng, J. , Xiao,J. & Lai, W. (1998). *Appl. Phys. Lett.* **72**, 1118–1120.
Xiao, J.Q., Jiang, J.S. & Chien, C.L. (1992). *Phys. Rev. Lett.* **68**, 3749–3752.
Yu, R.H., Zhang, X., Tejada, J., Zhu, J. & Knobel, M. (1996). *J. Appl. Phys.* **79**, 1979–1990.
Zabinsky, S.I., Rehr, J.J., Ankudinov, A., Albers, R.C. & Eller, M.J. (1995). *Phys. Rev. B* **52**, 2995–3009.
Zhang, S. & Levy, P.M. (1993). *J. Appl. Phys.* **73**, 5315–5319.

 Received 31 July 2000 • Accepted 3 January 2001